

Simulating enhanced modern heat transfer to the Arctic

J. H. Jungclaus et al.

This discussion paper is/has been under review for the journal Climate of the Past (CP). Please refer to the corresponding final paper in CP if available.

Enhanced 20th century heat transfer to the Arctic simulated in the context of climate variations over the last millennium

J. H. Jungclaus, K. Lohmann, and D. Zanchettin

Max Planck Institut für Meteorologie, Hamburg, Germany

Received: 16 June 2014 – Accepted: 25 June 2014 – Published: 14 July 2014

Correspondence to: J. H. Jungclaus (johann.jungclaus@mpimet.mpg.de)

Published by Copernicus Publications on behalf of the European Geosciences Union.

Title Page

Abstract

Introduction

Conclusions

References

Tables

Figures



Back

Close

Full Screen / Esc

Printer-friendly Version

Interactive Discussion



Abstract

Oceanic heat transport variations, carried by the northward flowing Atlantic Water, strongly influence Arctic sea-ice distribution, ocean–atmosphere exchanges, and pan-Arctic temperatures. Paleoceanographic reconstructions from marine sediments near Fram Strait have documented a dramatic increase in Atlantic Water temperatures over the 20th century, unprecedented in the last millennium. Here we present results from Earth system model simulations over the last millennium that reproduce and explain reconstructed integrated quantities such as pan-Arctic temperature evolution during the pre-industrial millennium as well as the exceptional Atlantic Water warming in Fram Strait in the 20th century. The associated increase in ocean heat transfer to the Arctic can be traced back to changes in the ocean circulation in the sub-polar North Atlantic. An interplay between a weakening overturning circulation and a strengthening sub-polar gyre as a consequence of 20th century global warming is identified as driving mechanism for the pronounced warming along the Atlantic Water path toward the Arctic. Simulations covering the late Holocene provide a reference frame that allows us to conclude that the changes during the last century are unprecedented in the last 1150 years and that they cannot be explained by internal variability or natural forcing alone.

1 Introduction

The Arctic is one of the regions where climate change has been diagnosed most drastically in terms of warming and sea-ice decline over the last decades. Direct temperature measurements are, however, scarce and only available for the last century. Reliable observations of sea-ice evolution are even more limited, covering only the satellite era. On decadal timescales, internal variations can substantially contribute to Arctic climate variability (Bengtsson et al., 2004; Beitsch et al., 2013) and the relative role of external drivers is still under debate (Booth et al., 2012; Zhang et al., 2013). High-resolution reconstructions of paleoclimatic variables over the late Holocene provide a reference

CPD

10, 2895–2924, 2014

Simulating enhanced modern heat transfer to the Arctic

J. H. Jungclaus et al.

Title Page

Abstract

Introduction

Conclusions

References

Tables

Figures



Back

Close

Full Screen / Esc

Printer-friendly Version

Interactive Discussion



Simulating enhanced modern heat transfer to the Arctic

J. H. Jungclaus et al.

Title Page

Abstract

Introduction

Conclusions

References

Tables

Figures



Back

Close

Full Screen / Esc

Printer-friendly Version

Interactive Discussion



frame and put recent changes in context with long-term natural variations. Ongoing efforts, such as the Past Global Changes 2K network (PAGES2K, Ahmed et al., 2013) initiative, provide regional syntheses of reconstructions that can be compared with model simulations. While most of the PAGES2K reconstructions rely on terrestrial proxies, high-quality marine paleodata become increasingly available at annual to decadal resolution. Novel proxies have been developed to reconstruct, for example, dynamical quantities such as near-bottom flow strength in the Nordic Seas overflow regions (e.g., Mjell et al., 2014). Of particular value are reconstructions from key locations, such as major conduits of the large-scale ocean circulation. Spielhagen et al. (2011) and Dylmer et al. (2013) have published records from marine sediments off Svalbard that reflect temperature changes in the Atlantic Water (AW) in Fram Strait over the last 2000–3000 years. The time series show centennial-scale modulations of the AW temperatures and, as a pronounced common feature, a dramatic, unprecedented warming over the 20th century. The authors speculate that the observed warming reflect considerable changes in the lateral heat transfer to the Arctic that might have contributed to the rapid warming and sea-ice decrease during the 20th century.

Earth system model simulations over the last millennium provide a tool to test such hypotheses, and to investigate the relative role of internal variability on the one hand, and natural and anthropogenic forcing on the other hand. Provided that the model adequately simulates regional-scale features, simulations also allow for attributing locally observed variations to changes in large-scale dynamics. In general, the model results have to be confronted with observations and reconstructions to assess in how far they reproduce the real climate evolution, both in direct comparison (e.g., Fernandez-Donado et al., 2012) and in a statistical sense (Bothe et al., 2013). In this paper, we use the results of Max Planck Institute Earth System Model (MPI-ESM) simulations for the last millennium and the industrial period to address the following research questions:

1. Can the simulations reproduce important features of reconstructed climate indicators in high northern latitudes during the last millennium and in the 20th century, both on a continental and local scale?

Simulating enhanced modern heat transfer to the Arctic

J. H. Jungclaus et al.

[Title Page](#)[Abstract](#)[Introduction](#)[Conclusions](#)[References](#)[Tables](#)[Figures](#)[Back](#)[Close](#)[Full Screen / Esc](#)[Printer-friendly Version](#)[Interactive Discussion](#)

The atmosphere model ECHAM6 (Stevens et al., 2013) is run at a horizontal resolution of spectral truncation T63 (1.875°) and 47 vertical levels, resolving the stratosphere up to 0.01 hPa. The ocean/sea-ice model MPIOM (Marsland et al., 2003; Jungclaus et al., 2013) features a conformal mapping grid with nominal 1.5° resolution and 40 vertical levels (GR1.5L40). It is noteworthy for our study that the GR1.5L40 grid possesses one grid pole over Antarctica and one grid pole over Greenland, which leads to considerably higher resolution in the regions of interest for this study, i.e. the northern North Atlantic (Jungclaus et al., 2008). In Fram Strait, for example, the grid size in cross-channel direction is about 30–40 km. The simulations over the last millennium (past1000) follow the protocol of the Paleo Modeling Intercomparison Project, phase 3 (PMIP3). As part of this protocol, Schmidt et al. (2011) summarize different choices for external forcing and boundary conditions and provide tables for well mixed-greenhouse gases (CO₂, CH₄, N₂O), and orbital parameters. In contrast to the millennium simulations described in Jungclaus et al. (2010), which featured an interactive carbon-cycle and prognostic CO₂, we use prescribed CO₂ in the past1000 runs described here. We employed the Crowley and Unterman (2013) reconstruction for volcanic aerosol optical depth and effective radius and the Pongratz et al. (2008) reconstruction of global land-cover and agricultural areas. For solar radiation we have followed the approach described in Schmidt et al. (2011) combining the Vieira et al. (2011) total solar irradiance (TSI) reconstruction over the Holocene with the Wang et al. (2005) data set that provides the recommended solar forcing for the CMIP5 20th century (1850–2005) simulations. An artificial 11 yr cycle of varying amplitude is imposed over the pre-industrial period (see Schmidt et al., 2011 for details). Linear interpolation was used to calculate monthly TSI averages from the reconstructed annual TSI values for the period 850–1849 scaled to Total Irradiance Monitor (TIM) data, except for the flux at 180.5 nm. Spectral Solar Irradiance (SSI) for the 14 short-wave spectral bands of the ECHAM6's radiation scheme was calculated so that the sum of SSI yields TSI. Energy in the part of the spectrum below the shortest wavelength of the radiation scheme (200 nm) and above the longest (12 195.1 nm) was added to the first and last band, respectively.

Simulating enhanced modern heat transfer to the Arctic

J. H. Jungclaus et al.

[Title Page](#)[Abstract](#)[Introduction](#)[Conclusions](#)[References](#)[Tables](#)[Figures](#)[Back](#)[Close](#)[Full Screen / Esc](#)[Printer-friendly Version](#)[Interactive Discussion](#)

Monthly average ozone concentrations for the period 850–1849 are calculated using the 1850–1860 monthly climatology of ozone concentrations from the AC&C/SPARC Ozone Database as a basis and representing the ozone dependency on solar irradiance through regression coefficients between historical ozone concentrations and the annual 180.5 nm solar flux. An 1155 year-long pre-industrial control integration (PiCtrl) under fixed 1850 boundary conditions serves as a reference simulation for forced experiments. To conduct the past1000 simulations we first ran a 400 year-long adaptation simulation starting from the end of piCtrl to adjust to 850 boundary conditions and thereafter started the three realizations past1000-r1, past1000-r2, and past1000-r3. The past1000-r1 and past1000-r2 experiments were initialized with the same ocean state, but differ in the standard deviation of the assumed lognormal distribution of the volcanic aerosol size (1.2 μm in r1, 1.8 μm in r2 and r3). The simulations past1000-r2 and past1000-r3 used the same parameter setting but were started from different initial conditions. Furthermore, ozone concentration data used in past1000-r1 are affected by use of a 1 month-shifted annual cycle in the AC&C/SPARC ozone climatology, an issue solved in past1000-r2 and -r3. While the three simulations are therefore not an ensemble of three runs carried out with an identical model and forcing/boundary conditions, we consider the effect of the different setting small enough to regard the runs as three realizations of possible last millennium climate evolution under parameter and forcing uncertainties. The PMIP3 protocol defines the past1000 integration period as 850–1849. To relate the recent climate evolution to the late-Holocene variability we continued the respective past1000 simulations over the historical period (1850–2005), following the CMIP5 protocol. In the following, we refer to the combined past1000 and historical simulations covering the period 850–2005 as pr1, pr2, and pr3, respectively. Since the emphasis of our present study is on the 20th century changes, we also include in some analyses in Sects. 4 and 5 one additional “historical” (hr1) simulation (1850–2005), which was initialized from the PiCtrl experiment.

3 Last millennium evolution of high northern latitude climate

3.1 Pan-Arctic temperature and sea-ice extent

We start the analyses with quantities that reflect the general climate evolution in high northern latitudes. Reconstructing regional-scale temperature and other climate variables such as sea-ice extent in sparsely-sampled areas is still challenging. Only recently pan-Arctic reconstructions for temperature have been published (Kaufman et al., 2009; Shi et al., 2012), mostly based on terrestrial proxies (tree-rings) and ice cores. The PAGES2K consortium reviewed reconstruction data and methods and constructed seven continental-scale temperature records, including the Arctic (Ahmed et al., 2013). The reconstructed temperature records (black lines in Fig. 1a) have in common that they show a gradual cooling during the last millennium, possibly reflecting the overall evolution from a warmer Medieval Warm Period (MWP) to an anomalously cold Little Ice Age (LIA), but the Shi et al. (2012) and Kaufman et al. (2009) reconstructions disagree on the magnitude of the pre-industrial cooling. The reconstructions (and the instrumental data that they are matched to) show a strongly reversed trend during the 20th century. Note that the PAGES2K record reflects annual mean temperatures whereas the other two represent the summer season. The simulated summer temperatures are compatible with the reconstructions and match closely the Kaufman et al. (2009) data. Individual simulations (colored lines in Fig. 1a) show relatively strong fluctuations and ensemble realizations differ often quite strongly (about 0.5°C) for a given period. In contrast to global and hemispheric averages (not shown here, but see Jungclaus et al., 2010: their Fig. 5), individual volcanic eruptions or clusters of volcanic events are not clearly discernible, with the exception of the 1809 and 1815 (Tambora) eruptions, where all simulations show a similar cold excursion, in accordance with the Kaufman and Past2K reconstructions. The resilience to volcanic forcing reflects the relatively small signal-to-noise ratio of Arctic summer temperatures, due to both strong internal variability of the Arctic regional climate (e.g. Beitsch et al., 2013) and seasonal character of local response mechanisms, which are most prominent in

Simulating enhanced modern heat transfer to the Arctic

J. H. Jungclaus et al.

Title Page

Abstract

Introduction

Conclusions

References

Tables

Figures



Back

Close

Full Screen / Esc

Printer-friendly Version

Interactive Discussion



boreal winter (e.g., Zanchettin et al., 2012, 2013). The Arctic warming throughout the 20th century is also well reflected in the model simulations and the pronounced variations such as the warm phase in the first half of the last century are well within the ensemble range of the historical experiments.

The summer sea-ice reconstruction by Kinnard et al. (2011) comes with a relatively large range of uncertainty but the main characteristic is that of a mirror-image of the pan-Arctic surface temperature evolution: a gradual increase in sea-ice extent during the pre-industrial millennium is replaced by a drastic decline in the 20th century (Fig. 1b). The decline of sea-ice extent sets in, however, more abruptly in the mid-20th century in contrast to the relatively gradual warming. The past1000 simulations reproduce a similar long-term trend over the pre-industrial millennium and the 20th century simulations terminate at an extent that is equally low as the observations. In the simulations, the sea-ice decline begins, however, earlier featuring a temporal evolution more similar to the pan-Arctic temperature (Fig. 1a). In fact, all four historical simulations show ice extent anomalies below the reconstruction's mean estimate between 1870 and 1950. None of the three past1000 simulations reproduces the sea-ice minimum in the late 16th century. Notwithstanding questions regarding uncertainties in the reconstructions, the anomaly exceeds the 2-sigma range of control experiment variability not by too far, so that it is compatible with a rare event of internal fluctuations.

3.2 Fram Strait Atlantic Water temperatures

The reconstructions of AW temperatures stem from a marine core at site MSM5/5-712 at 78°54.94' N, 6°46.04' E (see Spielhagen et al. (2011) and Werner et al. (2011) for details). The authors provide two temperature records, one based on a modern analogue technique (SIMMAX), and one based on the Magnesium–Calcium (Mg/Ca) ratio of *Neogloboquadrina pachyderma*. Habitat and plankton bloom estimates indicate that both proxies reflect mid-summer conditions in the upper part of the AW layer. During pre-industrial times, the Mg/Ca-derived record exhibits much stronger variability, which might reflect inaccuracies in recording the cold-water range (Spielhagen et al., 2011).

Simulating enhanced modern heat transfer to the Arctic

J. H. Jungclaus et al.

Title Page

Abstract

Introduction

Conclusions

References

Tables

Figures



Back

Close

Full Screen / Esc

Printer-friendly Version

Interactive Discussion



Simulating enhanced modern heat transfer to the Arctic

J. H. Jungclaus et al.

Title Page

Abstract

Introduction

Conclusions

References

Tables

Figures



Back

Close

Full Screen / Esc

Printer-friendly Version

Interactive Discussion



conduits towards the Arctic. The correlation coefficients between AW temperatures and TOHTR (smoothed by a 31 yr running mean) exceed 0.9 at zero time-lag in all three past1000 simulations. Simulated TOHTR anomalies are shown with respect to (w.r.t.) the pre-industrial (850–1849) mean of about 80 TW (1 TW = 10^{12} Watt). The simulated transports are compatible with observations indicating a heat transport of 30–40 TW in Fram Strait (Schauer et al., 2008) and 30–76 TW in BSO (Årthun et al., 2012). Observations of heat transports are, however, only available for the most recent decades and may be influenced by decadal-scale variability as well. During the pre-industrial period, there are TOHTR fluctuations of the order of 10–20 TW and the ensemble indicates somewhat higher-than-normal TOHTR in the early part of the simulation and less TOHTR in the 16th and 17th century. Large volcanic eruptions (1258, 1453, and 1815) leave an imprint on the heat transports leading to reduction of heat transfer to the Arctic (Zanchettin et al., 2012). The most pronounced feature of our smoothed time series from the simulations is, however, a consistent increase of up to 30 TW during the 20th century, reflecting a 40 % increase over the pre-industrial mean.

The modulation of the AW temperature could either be driven by local changes in the wind system (Bengtsson et al., 2004) or be part of variations in the warm water path associated with the North Atlantic Current or the Atlantic Meridional Overturning Circulation (AMOC), as has been suggested, for example by Polyakov et al. (2004). However, recently Lozier (2010) and Lozier et al. (2010) have demonstrated that overturning and gyre circulation in the North Atlantic are strongly linked and that the image of a continuous conveyor belt associated with the AMOC may be misleading. Building on earlier results analyzing Arctic warming events in an unperturbed control integration (Beitsch et al., 2013) we therefore decompose the (TOHTR) in the Atlantic basin into its overturning and gyre components (MOHTR, and GOHTR, respectively). The first reflects the zonal average heat transport, the second the deviations of the zonal average (e.g. Eden and Jung, 2001; Drijfhout and Hazeleger, 2006). First, we calculate the correlations between the TOHTR at the entrance to the Arctic (Fig. 2a) and the components of the basin-scale OHTRs for all latitudes. High correlations are found in particular in the

Simulating enhanced modern heat transfer to the Arctic

J. H. Jungclaus et al.

Title Page

Abstract

Introduction

Conclusions

References

Tables

Figures



Back

Close

Full Screen / Esc

Printer-friendly Version

Interactive Discussion



The OHTR trends discussed here reflect changes in the large-scale ocean circulation. The AMOC decreases particularly in the sub-tropical and most of the sub-polar North Atlantic, while its branch reaching into the Nordic Seas increases in strength (Fig. 5a). The sub-polar gyre (SPG) increases in strength mainly in the eastern part of the basin, while it slightly decreases in the central Labrador Sea (Fig. 5b, shown here for experiment pr2, but similar for the other simulations). The weakening of the overturning circulation is associated with a decrease of Labrador Sea Water formation. At the eastern exit of the Labrador Sea, temperature and density changes imply that mid-depth reaching convection in the Labrador Sea decreases (Fig. 6). At the same time, the deepest layers get colder and denser owing to somewhat colder overflows. Changes in the vertical density structure are important for the east-west density gradient driving the AMOC (Lozier et al., 2010), but also affect the baroclinic structure of the gyre directly (Drijfhout and Hazeleger, 2006).

5 Discussion

Our analysis has demonstrated that the increasing heat transports to higher latitudes are mainly caused by changes in SPG circulation. We propose that the SPG change is a response to a weakening of the AMOC and the associated reduced heat supply (MOHTR, blue lines in Fig. 3a) from the south. The colder and denser SPG then spins up baroclinically, which further increases the GOHTR (red lines in Fig. 3a), which, in turn, extracts even more heat from the SPG center and further increases the horizontal density gradient. Thus a positive feedback mechanism is initiated. The mechanism can be compared to the one described by Levermann and Born (2007) and Born et al. (2013a). These authors describe a positive feedback, where an (somehow) accelerated gyre leads to increasing east-west temperature and salt transports along its northern rim. Increasing salinity then leads to denser surface waters in the Labrador Sea and to enhanced convective activity, which further spins up the gyre. In our simulations, we see also a redistribution of salinity during the 20th century change in gyre circulation

Simulating enhanced modern heat transfer to the Arctic

J. H. Jungclaus et al.

Title Page

Abstract

Introduction

Conclusions

References

Tables

Figures



Back

Close

Full Screen / Esc

Printer-friendly Version

Interactive Discussion



resulting in higher salinities in the western part of the basin. However, in contrast to the mechanism described by Levermann and Born (2007), the positive temperature anomalies dominate the near-surface density evolution and Labrador Sea convection rather decreases. Levermann and Born (2007) demonstrated that a bistability regime exists, where the transition between the two regimes can be triggered by small fluctuations in surface freshwater flux. Born et al. (2013a) extended the study and found multiple circulation modes in PiCtrl experiments in six out of 19 models (among them MPI-ESM-LR). Even though we find some differences to their mechanism, it is possible that the relatively strong response of the SPG is an expression of such a transition, here triggered by changes in the AMOC. Possibly also the wind-stress changes (Fig. 4) play a role in initiating the change in the gyre circulation by modified Ekman and/or Sverdrup transports. It is difficult, however, to exactly detect which component is more important. For this, additional sensitivity experiments (e.g., partial-coupling experiments) would be necessary, which is beyond the scope of this study. In any case, an important ingredient is the weakening of the AMOC in subtropical and subpolar latitudes, caused by a decrease in Labrador Sea Water formation as a response to global warming, while the deep water production in the Nordic Seas is even slightly enhanced. The exact mechanisms of how gyre and overturning circulations interact are also difficult to disentangle. In the historical simulations, changes in AMOC and SPG circulation appear to happen more or less instantaneous, whereas analyses of the unperturbed control simulation suggest that AMOC variations are leading by a few years. Furthermore, gyre circulation changes can also directly be driven by changes in the baroclinic structure at the western boundary as has been shown in the global warming simulations by Drijfhout and Hazeleger (2006). At the western boundary near the exit of the Labrador Sea (Fig. 6), the density changes are consistent with a weakening of Labrador Sea Water production and an increase in overflow-derived density, similar to what has been found by Drijfhout and Hazeleger (2006).

Many CMIP5 models feature a reduction of the AMOC strength already in the 20th century (Drijfhout et al., 2012). A characteristic feature of these simulations is the

“warming hole” above the sub-polar North Atlantic that can also be identified in observations (e.g. in the HadSST data set; Rayner et al., 2006). A cool surface temperature spot within the intensified SPG is also characteristic for our 20th century simulations (Fig. 3c) and clearly related to the mechanism described above. Drijfhout et al. (2012) decompose the temperature pattern in a radiatively forced and an AMOC fingerprint and conclude that the cold sub-polar North Atlantic is indeed related to an AMOC decline. Kim and An (2012) come to a similar conclusion analyzing CO₂-doubling experiments from the Coupled Model Intercomparison Project Phase 3 data base. Another indication that the mechanism described here is at work in reality comes from paleoceanographic reconstructions for the late Holocene. Mietinnen et al. (2012) compare the temporal evolution of ocean temperatures at two locations, the Voering Plateu in the Norwegian Sea and the SPG region south of the Rejkjanes Ridge. They find that low-frequency fluctuations occur out-of-phase: the Voering Plateau record features, for example, a cold anomaly during the Little Ice Age (LIA), whereas the SPG is warmer than normal during this period. Such a behavior is compatible with the findings described here: a weaker SPG in the LIA (Fig. 2) would feature a less dense and warmer center (opposite to what is seen for the strong-gyre anomaly in Fig. 3c) and would transport less heat to the Nordic Seas. Such out-of-phase anomalies of the barotropic stream function in the SPG region and the Nordic Seas can also be seen in Fig. 5b. A detailed investigation of the variations and processes during the pre-industrial millennium and their relation to natural forcing will be subject of a subsequent study.

While the dynamical mechanisms proposed here to explain the enhanced heat transfer to the Arctic are compatible with observed features in the North Atlantic, they may depend on the particular model system. Moreover, as many other CMIP5 models, MPI-ESM features large SST and circulation biases in the North Atlantic. In particular, the path of the Gulf Stream/North Atlantic Current is too zonal (Jungclaus et al., 2013), which has direct consequences for the shape of the gyres. This may affect the warm water path from the Subtropics to the Nordic Seas. Using observations and model simulations for the second half of the 20th century, Hatún et al. (2005) concluded that

CPD

10, 2895–2924, 2014

Simulating enhanced modern heat transfer to the Arctic

J. H. Jungclaus et al.

Title Page

Abstract

Introduction

Conclusions

References

Tables

Figures



Back

Close

Full Screen / Esc

Printer-friendly Version

Interactive Discussion



Simulating enhanced modern heat transfer to the Arctic

J. H. Jungclaus et al.

Title Page

Abstract

Introduction

Conclusions

References

Tables

Figures



Back

Close

Full Screen / Esc

Printer-friendly Version

Interactive Discussion



a weaker (and less zonally-extended) SPG would allow more warm and saline water to enter the Nordic Seas. Our simulations, but also other CMIP5 ESMs (Born et al., 2013a; Koenigk and Brodeau, 2014) and stand-alone ocean model simulations with the same ocean model as used here, but forced by reanalysis data (Müller et al., 2014) suggest that a stronger SPG carries more subtropical AW into the Nordic Seas and the Arctic. This discrepancy may be related to the specific situation of the late 20th century described by Hatún et al. (2005), where SPG changes were mainly related to the atmospheric forcing (Häkkinen and Rhines, 2009; see also Born et al., 2013b).

A 30 TW increase in heat transfer to the Arctic over 100 years as suggested by our simulations for the 20th century is an important contribution to the Arctic heat budget (Serreze et al., 2007). Dividing by the area of the Arctic, it corresponds to a substantial forcing of about 2 W m^{-2} . Jungclaus and Koenigk (2010) and Beitsch et al. (2013) have shown that multidecadal variations in TOHTR to the Arctic impact the Arctic climate. For positive TOHTR anomalies, the sea-ice cover decreases most pronounced in the Barents Sea and causes considerable variations in ocean–atmosphere heat fluxes. Although only a small fraction of the Arctic is affected, the associated warming leads to positive pan-Arctic temperature anomalies. Moreover, the heat-flux changes affect the atmospheric circulation. An associated feedback mechanism is the Bjerknes Compensation (Bjerknes, 1964; Shaffrey and Sutton, 2006; Jungclaus and Koenigk, 2010): on multidecadal time-scales, TOHTR and atmospheric heat transports (AHTR, here derived from the components of moist and dry static energy advection following Keith, 1995) are strongly coupled and may compensate each other. Thus, both TOHTR and AHTR need to be considered for an assessment of the lateral heat transfer changes as part of the Arctic heat budget. Comparing TOHTR and AHTR at 70° N (Fig. 7) indicates considerable multidecadal variability where the respective TOHTR and AHTR tend to evolve out-of-phase. However, there is no compensation of the strong positive trend in TOHTR during the last decades of the simulation. Therefore we conclude that there is a net positive contribution from the lateral heat fluxes to the Arctic heat budget and to the warming in recent decades. An assessment of all terms of the Arctic heat bud-

get and the feedback mechanisms leading to Arctic Amplification is, however, beyond the scope of our paper. The magnitude of TOHTR changes appears to play a decisive role in the amplitude of pan-Arctic warming, and sea-ice evolution in climate-change simulations (Mahlstein and Knutti, 2011). These authors concluded that the TOHTR changes contribute significantly to Arctic amplification, but they also identified considerable differences in the TOHTR magnitude in the CMIP3-model suite as a cause for model uncertainty in projected Arctic warming.

6 Conclusions

The MPI-ESM last-millennium simulations consistently reproduce enhanced 20th century warming of AW at the boundary between the Nordic Seas and the Arctic compared with pre-industrial variability. The warming of AW in Fram Strait is an indicator for a prominent (~ 40 %) increase in oceanic heat transfer to the Arctic during the 20th century. In the simulations, we are able to trace back the heat transport changes to a reorganization of the large-scale ocean circulation in the sub-polar North Atlantic. The SPG and the associated northward heat transport are intensified by the global-warming-induced weakening of the AMOC and changes in the density structure associated with modified deep water formation. The latter also lead to a slight intensification of the overturning in high northern latitudes. Together, the gyre and overturning-related heat transport changes lead to an increase in the heat transfer to the Nordic Seas and the Arctic. Changes in wind-stress curl do not appear to be significantly different from the unperturbed variability, but wind-stress changes may nonetheless play a role in triggering the mechanism. Transient simulations over the late Holocene provide a valuable reference frame to discriminate unprecedented changes such as those observed in the 20th century from natural or internal fluctuations.

Simulating enhanced modern heat transfer to the Arctic

J. H. Jungclaus et al.

Title Page

Abstract

Introduction

Conclusions

References

Tables

Figures



Back

Close

Full Screen / Esc

Printer-friendly Version

Interactive Discussion



Acknowledgements. This work was supported by the European Community's 7th framework program (FP7/2007-2013) under grant agreement no. 308299 (NACLIM). D. Zanchettin was supported by the German Federal Ministry for Education and Research (BMBF) Miklip project (FKZ: 01LP1158A). The MPI-ESM-P simulations were conducted at the German Climate Computing Center (DKRZ). The authors thank Chao Li for comments that helped improving the manuscript.

The service charges for this open access publication have been covered by the Max Planck Society.

References

- Ahmed, M. and the PAGES 2k Consortium: Continental-scale temperature variability during the last two millennia, *Nat. Geosci.*, 6, 339–346, doi:10.1038/ngeo1797, 2013.
- Årthun, M., Eldevik, T., Smedsrud, L. H., Skagseth, Ø., Ingvaldsen, R. B.: Quantifying the influence of Atlantic heat on Barents Sea ice variability and retreat, *J. Climate*, 25, 4736–4743, doi:10.1175/JCLI-D-11-00466.1, 2013.
- Beitsch, A., Jungclaus, J. H., and Zanchettin, D.: Patterns of decadal-scale Arctic warming events in simulated climate, *Clim. Dynam.*, in press, doi:10.1007/s00382-013-2004-5, 2013.
- Bengtsson, L., Semenov, V. A., and Johannessen, O. M.: The early twentieth-century warming in the Arctic – a possible explanation, *J. Climate*, 18, 4045–4057, doi:10.1175/1520-0442(2004)017<4045:TETWIT>2.0.CO;2, 2004.
- Bjerknes, J.: Atlantic air–sea interaction, *Adv. Geophys.*, 10, 1–82, 1964.
- Booth, B. B. B., Dunstone, N. J., Halloran, P. R., Andrews, T., and Bellouin, N.: Aerosols implicated as a prime driver of twentieth century North Atlantic climate variability, *Nature*, 484, 228–232, doi:10.1038/nature10946, 2012.
- Born, A., Stocker, T. F., Raible, C. C., and Levermann, A.: Is the Atlantic subpolar gyre bistable in comprehensive climate models?, *Clim. Dynam.*, 40, 2993–3007, doi:10.1007/s00382-012-1525-7, 2013a.
- Born, A., Stocker, T. F., and Sandø, A. B.: Coupling of eastern and western subpolar North Atlantic: salt transport in the Irminger Current, *Ocean Sci. Discuss.*, 10, 555–579, doi:10.5194/osd-10-555-2013, 2013.

Simulating enhanced modern heat transfer to the Arctic

J. H. Jungclaus et al.

Title Page

Abstract

Introduction

Conclusions

References

Tables

Figures



Back

Close

Full Screen / Esc

Printer-friendly Version

Interactive Discussion



Simulating enhanced modern heat transfer to the Arctic

J. H. Jungclaus et al.

Title Page

Abstract

Introduction

Conclusions

References

Tables

Figures



Back

Close

Full Screen / Esc

Printer-friendly Version

Interactive Discussion



- Bothe, O., Jungclaus, J. H., and Zanchettin, D.: Consistency of the multi-model CMIP5/PMIP3-past1000 ensemble, *Clim. Past*, 9, 2471–2487, doi:10.5194/cp-9-2471-2013, 2013.
- Crowley, T. J. and Unterman, M. B.: Technical details concerning development of a 1200 yr proxy index for global volcanism, *Earth Syst. Sci. Data*, 5, 187–197, doi:10.5194/essd-5-187-2013, 2013.
- 5 Drijfhout, S. S. and Hazeleger, W.: Changes in MOC and gyre-induced Atlantic Ocean heat transport, *Geophys. Res. Lett.*, 33, L07707, doi:10.1029/2006GL025807, 2006.
- Drijfhout, S., van Oldenborgh, G. J., and Cimadoribus, A.: Is a decline of AMOC causing the warming hole above the North Atlantic in observed and modeled warming patterns?, *J. Climate*, 25, 8373–8379, doi:10.1175/JCLI-D-12-00490.1, 2012.
- 10 Dylmer, C. V., Giraudeau, J., Eynaud, F., Husum, K., and De Vernal, A.: Northward advection of Atlantic water in the eastern Nordic Seas over the last 3000 yr, *Clim. Past*, 9, 1505–1518, doi:10.5194/cp-9-1505-2013, 2013.
- Eden, C. and Jung, T.: North Atlantic interdecadal variability: oceanic response to the North Atlantic Oscillation (1865–1997), *J. Climate*, 14, 676–691, 2001.
- Fernández-Donado, L., González-Rouco, J. F., Raible, C. C., Ammann, C. M., Barriopedro, D., García-Bustamante, E., Jungclaus, J. H., Lorenz, S. J., Luterbacher, J., Phipps, S. J., Servonnat, J., Swingedouw, D., Tett, S. F. B., Wagner, S., Yiou, P., and Zorita, E.: Large-scale temperature response to external forcing in simulations and reconstructions of the last millennium, *Clim. Past*, 9, 393–421, doi:10.5194/cp-9-393-2013, 2013.
- 20 Giorgetta, M. A., Jungclaus, J. H., Reick, C. H., Legutke, S., Brovkin, V., Cruieger, T., Esch, M., Fieg, K., Glushak, K., Gayler, V., Haak, H., Hollweg, H.-D., Ilyina, T., Kinne, S., Kornblueh, L., Matei, D., Mauritsen, T., Mikolajewicz, U., Mueller, W. A., Notz, D., Raddatz, T., Rast, S., Redler, R., Roeckner, E., Schmidt, H., Schnur, R., Segschneider, J., Six, K., Stockhause, M., Wegner, J., Widmann, H., Wieners, K.-H., Claussen, M., Marotzke, J., and Stevens, B.: Climate and carbon cycle changes from 1850 to 2100 in MPI-ESM simulations for the Coupled Model Intercomparison Project phase 5, *J. Adv. Model Earth Syst.*, 5, 1–26, doi:10.1002/jame.20038, 2013.
- 25 Greatbatch, R., Fanning, A., Goulding, A., and Levitus, S.: A diagnosis of interpentadal circulation changes in the North Atlantic, *J. Geophys. Res.*, 96, 22009–22023, 1991.
- 30 Häkkinen, S. and Rhines, P. B.: Shifting surface currents in the northern North Atlantic, *J. Geophys. Res.*, 114, C04005, doi:10.1029/2008JC004883, 2009.

Simulating enhanced modern heat transfer to the Arctic

J. H. Jungclaus et al.

[Title Page](#)

[Abstract](#)

[Introduction](#)

[Conclusions](#)

[References](#)

[Tables](#)

[Figures](#)



[Back](#)

[Close](#)

[Full Screen / Esc](#)

[Printer-friendly Version](#)

[Interactive Discussion](#)



Hald, M., Salomonsen, G. R., Husum, K., and Wilson, L. J.: A 2000 year record of Atlantic Water temperature variability from Malangen Fjord, northeastern North Atlantic, The Holocene, 21, 1049–1059, doi:10.1177/0959683611400457, 2011.

Hátún, H., Sandø, A. B., Drange, H., Hansen, B., and Valdimarsson, H.: Influence of the Atlantic subpolar gyre on the thermohaline circulation, *Science*, 309, 1841–1844, doi:10.1126/science.1114777, 2005.

Jungclaus, J. H. and Koenigk, T.: Low-frequency variability of the Arctic climate: the role of oceanic and atmospheric heat transport variations, *Clim. Dynam.*, 34, 265–279, doi:10.1007/s00382-009-0569-9, 2010.

Jungclaus, J. H., Macrander, A., and Käse, R. H.: Modelling the overflow across the Greenland–Scotland Ridge, in: *Arctic–Subarctic Ocean Fluxes*, edited by: Dickson, R. R., Meincke, J., and Rhines, P., Springer, Dordrecht, 527–549, 2008.

Jungclaus, J. H., Lorenz, S. J., Timmreck, C., Reick, C. H., Brovkin, V., Six, K., Segschneider, J., Giorgetta, M. A., Crowley, T. J., Pongratz, J., Krivova, N. A., Vieira, L. E., Solanki, S. K., Klocke, D., Botzet, M., Esch, M., Gayler, V., Haak, H., Raddatz, T. J., Roeckner, E., Schnur, R., Widmann, H., Claussen, M., Stevens, B., and Marotzke, J.: Climate and carbon-cycle variability over the last millennium, *Clim. Past*, 6, 723–737, doi:10.5194/cp-6-723-2010, 2010.

Jungclaus, J. H., Fischer, N., Haak, H., Lohmann, K., Marotzke, J., Matei, D., Mikolajewicz, U., Notz, D., and von Storch, J.-S.: Characteristics of the ocean simulations in the Max Planck Institute Ocean Model (MPIOM) the ocean component of the MPI-Earth system model, *J. Adv. Model Earth Syst.*, 5, 422–446, doi:10.1002/jame.20023, 2013.

Kaufman, D. S., Schneider, D. P., McKay, N. P., Ammann, C. M., Bradley, R. S., Briffa, K. R., Miller, G. H., Otto-Bliesner, B. L., Overpeck, J. T., Vinther, B. M., and Arctic Lakes 2K project members: recent warming reverses long-term Arctic cooling, *Science*, 325, 1236–1239, doi:10.1126/science.1173983, 2009.

Keith, D. W.: Meridional energy transport: uncertainty in zonal means, *Tellus A*, 47, 30–44, 1995.

Kim, H. and An, S.-I.: On the subarctic North Atlantic cooling due to global warming, *Theor. Appl. Climatol.*, 114, 1–19, doi:10.1007/s00704-012-0805-9, 2012.

Kinnard, C., Zdanowicz, C. M., Fisher, D. A., Isaksson, E., De Vernal, A., and Thompson, L. G.: Reconstructed changes in Arctic sea ice over the last 1,450 years, *Nature*, 479, 509–513, doi:10.1038/nature10581, 2011.

Simulating enhanced modern heat transfer to the Arctic

J. H. Jungclaus et al.

Title Page

Abstract

Introduction

Conclusions

References

Tables

Figures



Back

Close

Full Screen / Esc

Printer-friendly Version

Interactive Discussion



Koenigk, T. and Brodeau, L.: Ocean heat transport into the Arctic in the twentieth and twenty-first century in EC-Earth, *Clim. Dynam.*, 42, 3101–3120, doi:10.1007/s00382-013-1821-x, 2014.

Levermann, A. and Born, A.: Bistability of the Atlantic subpolar gyre in a coarse-resolution climate model, *Geophys. Res. Lett.*, 34, L24605, doi:10.1029/2007GL031732, 2007.

Lozier, M. S.: Deconstructing the Conveyor Belt, *Science*, 328, 1507–1511, doi:10.1126/science.1189250, 2010.

Lozier, M. S., Roussenov, V., Reed, M. S. C., and Williams, R. G.: Opposing decadal changes for the North Atlantic meridional overturning circulation, *Nat. Geosci.*, 3, 728–734, doi:10.1038/NGEO947, 2010.

Mahlstein, I. and Knutti, R.: Ocean heat transport as a cause for model uncertainty in projected Arctic warming, *J. Climate*, 24, 1451–1460, doi:10.1175/JCLI3713.1, 2011.

Marsland, S. J., Haak, H., Jungclaus, J. H., Latif, M., and Roeske, F.: The Max-Planck-Institute global ocean/sea-ice model with orthogonal curvilinear coordinates, *Ocean Model.*, 5, 91–127, 2003.

Miettinen, A., Divine, D., Koç, N., Godtliobsen, F., and Hall, I. R.: Multicentennial variability of the sea surface temperature gradient across the subpolar North Atlantic over the last 2.8 kyr, *J. Climate*, 25, 4205–4219, doi:10.1175/JCLI-D-11-00581.1, 2012.

Mjell, T. L., Ninnemann, H. F., Kleiven, H. F., and Hall, I. R.: Multidecadal changes in Iceland–Scotland overflow water vigor over the last 600 years and its relation to climate, *Geophys. Res. Lett.*, in review, 2014.

Müller, W. A., Matei, D., Bersch, M., Jungclaus, J. H., Haak, H., Lohmann, K., Compo, G. P., Sardeshmukh, P. D., and Marotzke, J.: A 20th century reanalysis-forced ocean model to reconstruct the North Atlantic climate variations during the 1920s, *Clim. Dynam.*, accepted, 2014.

Pavlov, A., Tverberg, V., Ivanov, B., Nilsen, F., Falk-Petersen, S., and Granskog, M.: Warming of Atlantic Water in two west Spitsbergen fjords over the last century (1912–2009), *Polar Res.*, 32, 11206, doi:10.3402/polar.v32i0.11206, 2013.

Polyakov, I. V., Alekseev, G. V., Timokhov, L. A., Bhatt, U. S., Colony, R. L., Simmons, H. L., Walsh, D., Walsh, J. E., and Zakharov, V. F.: Variability of the Intermediate Atlantic Water of the Arctic Ocean over the last 100 years, *J. Climate*, 17, 4485–4497, 2004.

Simulating enhanced modern heat transfer to the Arctic

J. H. Jungclaus et al.

Title Page

Abstract

Introduction

Conclusions

References

Tables

Figures



Back

Close

Full Screen / Esc

Printer-friendly Version

Interactive Discussion



Pongratz, J., Reick, C. H., Raddatz, T., and Claussen, M.: A reconstruction of global agricultural areas and land cover for the last millennium, *Global Biogeochem. Cy.*, 22, GB3018, doi:10.1029/2007GB003153, 2008.

Rayner, N. A., Brohan, P., Parker, D. E., Folland, C. K., Kennedy, J. J., Vanicek, M., Ansell, T. J., and Tett, S. F. B.: Improved analyses of changes and uncertainties in sea surface temperature measured in situ since the mid nineteenth century: the HadSST2 data set, *J. Climate*, 19, 446–469, doi:10.1175/jcli3637.1, 2006.

Saenko, O. A., Fyfe, J. C., and England, M. H.: On the response of the oceanic wind-driven circulation to atmospheric CO₂ increase, *Clim. Dynam.*, 25, 415–426, doi:10.1007/s00382-005-0032-5, 2005.

Schauer, U., Beszynnka-Möller, A., Walczowski, W., Fahrbach, E., Piechura, J., and Hansen, E.: Variations of measured heat flow through Fram Strait between 1997 and 2006, in: *Arctic–Subarctic Ocean Fluxes*, edited by: Dickson, R. R., Meincke, J., and Rhines, P., Springer, Dordrecht, 65–85, 2008.

Schmidt, G. A., Jungclaus, J. H., Ammann, C. M., Bard, E., Braconnot, P., Crowley, T. J., Delaygue, G., Joos, F., Krivova, N. A., Muscheler, R., Otto-Bliesner, B. L., Pongratz, J., Shindell, D. T., Solanki, S. K., Steinhilber, F., and Vieira, L. E. A.: Climate forcing reconstructions for use in PMIP simulations of the last millennium (v1.0), *Geosci. Model Dev.*, 4, 33–45, doi:10.5194/gmd-4-33-2011, 2011.

Serreze, M. C., Barnett, A. P., Slater, A. G., Steele, M., Zhang, J., and Trenberth, K. E.: The large-scale energy budget of the Arctic, *J. Geophys. Res.*, 112, D11122, doi:10.1029/2006JD008230, 2007.

Sedlacek, J. and Mysak, L. A.: A model study of the Little Ice Age and beyond: changes in ocean heat content, hydrography and circulation since 1500, *Clim. Dynam.*, 33, 461–475, 2009.

Shaffrey, L. and Sutton, R.: Bjerknes compensation and the decadal variability of the energy transports in a coupled climate model, *J. Climate*, 19, 1167–1448, doi:10.1175/JCLI3652.1, 2006.

Shi, F., Yang, B., Ljungqvist, F. C., and Yang, F.: Multi-proxy reconstruction of Arctic summer temperatures over the past 1400 years, *Clim. Res.*, 54, 113–128, doi:10.3354/cr01112, 2012.

Simulating enhanced modern heat transfer to the Arctic

J. H. Jungclaus et al.

[Title Page](#)

[Abstract](#)

[Introduction](#)

[Conclusions](#)

[References](#)

[Tables](#)

[Figures](#)



[Back](#)

[Close](#)

[Full Screen / Esc](#)

[Printer-friendly Version](#)

[Interactive Discussion](#)



Spielhagen, R. F., Wagner, K., Sørensen, S. A., Zamelczyk, K., Kandiano, E., Budeus, G., Husum, K., Marchitto, T. M., and Hald, M.: Enhanced modern heat transfer to the Arctic by warm Atlantic Water, *Science*, 331, 450–453, doi:10.1126/science.1197397, 2011.

Stevens, B., Giorgetta, M., Esch, M., Mauritsen, T., Crueger, T., Rast, S., Salzmann, M., Schmidt, H., Bader, J., Block, K., Brokopf, R., Fast, I., Kinne, S., Kornblueh, L., Lohmann, U., Pincus, R., Reichler, T., and Roeckner, E.: Atmospheric component of the MPI-M Earth System Model: Echam6, *J. Adv. Model Earth Syst.*, 5, 146–172, doi:10.1002/jame.20015, 2013.

Vieira, L. E. A., Solanki, S. K., Krivova, N. A., and Usoskin, I.: Evolution of the solar irradiance during the Holocene, *Astron. Astrophys.*, 531, 20 pp., A6, doi:10.1051/0004-6361/201015843, 2011.

Wang, Y.-M., Lean, J. L., and Sheeley Jr., N. R.: Modeling the Sun's magnetic field and irradiance since 1713, *Astrophys. J.*, 625, 522–538, doi:10.1086/429689, 2005.

Werner, K., Spielhagen, R. F., Bauch, D., Hass, H. C., Kandiano, E., and Zamelczyk, K.: Atlantic water advection to the eastern Fram Strait – multiproxy evidence for late Holocene variability, *Paleogeogr. Paleoclimatol.*, 308, 264–276, doi:10.1016/j.palaeo.2011.05.030, 2011.

Zanchettin, D., Timmreck, C., Graf, H.-F., Rubino, A., Lorenz, S., Lohmann, K., Krüger, K., and Jungclaus, J. H.: Bi-decadal variability excited in the coupled ocean–atmosphere system by strong tropical volcanic eruptions, *Clim. Dynam.*, 39, 419–444, doi:10.1007/s00382-011-1167-1, 2012.

Zanchettin, D., Timmreck, C., Bothe, O., Lorenz, S. J., Hegerl, G., Graf, H.-F., Luterbacher, J., and Jungclaus, J. H.: Delayed winter warming: a robust decadal response to strong tropical volcanic eruptions?, *Geophys. Res. Lett.*, 40, 204–209, doi:10.1029/2012GL054403, 2013.

Zhang, R., Delworth, T. L., Sutton, R., Hodson, D. L. R., Dixon, K. W., Held, I. M., Kushnir, Y., Marshall, J., Ming, Y., Msadek, R., Robson, J., Rosati, A. J., Ting, M. F., and Vecchi, G.: Have aerosols caused the observed Atlantic multidecadal variability?, *J. Atmos. Sci.*, 70, 1135–1144, doi:10.1175/JAS-D-12-0331.1, 2013.

Simulating enhanced modern heat transfer to the Arctic

J. H. Jungclaus et al.

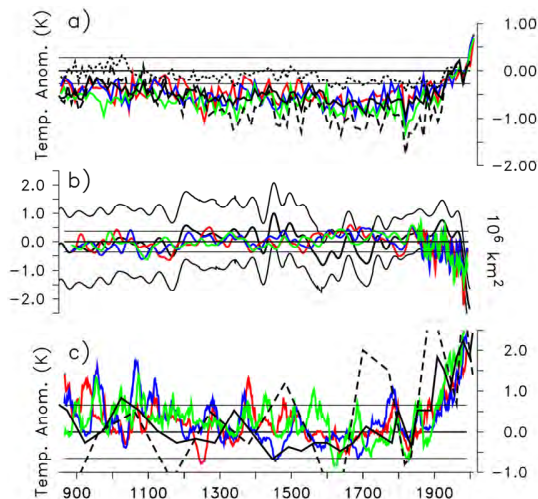


Figure 1. Simulated time series (colored lines for experiments pr1, pr2, pr3) of high northern latitude climate variables in comparison with reconstructions (black lines): **(a)** 10 year averages of Arctic summer (JJA) surface air temperatures as anomalies w.r.t. the 1960–1990 mean. Summer temperature reconstructions are from: (solid black) Kaufman et al. (2009), and (dotted black) Shi et al. (2012). The PAGES2K reconstruction representing annual temperatures is also shown (dashed black). **(b)** late-summer (August) sea-ice extent (in 10^6 km^2) as anomalies w.r.t. the pre-industrial mean in comparison with the reconstruction by Kinnard et al. (2011): the thick black line denotes the 40 year smoothed reconstruction, the thin black lines the 95 % confidence interval; for the simulations, a 41 yr running mean was applied for pre-industrial millennium and a 5 yr running mean for 1850–2005 to better display 20th century variability. **(c)** Atlantic Water temperature anomalies w.r.t. the pre-industrial mean in Fram Strait (78° N , 50 m depth) in comparison with the reconstruction by Spielhagen et al. (2011) obtained by the (solid black) SIMMAX, and (dashed black) Mg/Ca methods, respectively. In all plots, thin horizontal lines bracketing the zero line indicate the respective 2σ -ranges derived from the 1000 yr-long PiCtrl experiment.

Title Page

Abstract

Introduction

Conclusions

References

Tables

Figures



Back

Close

Full Screen / Esc

Printer-friendly Version

Interactive Discussion



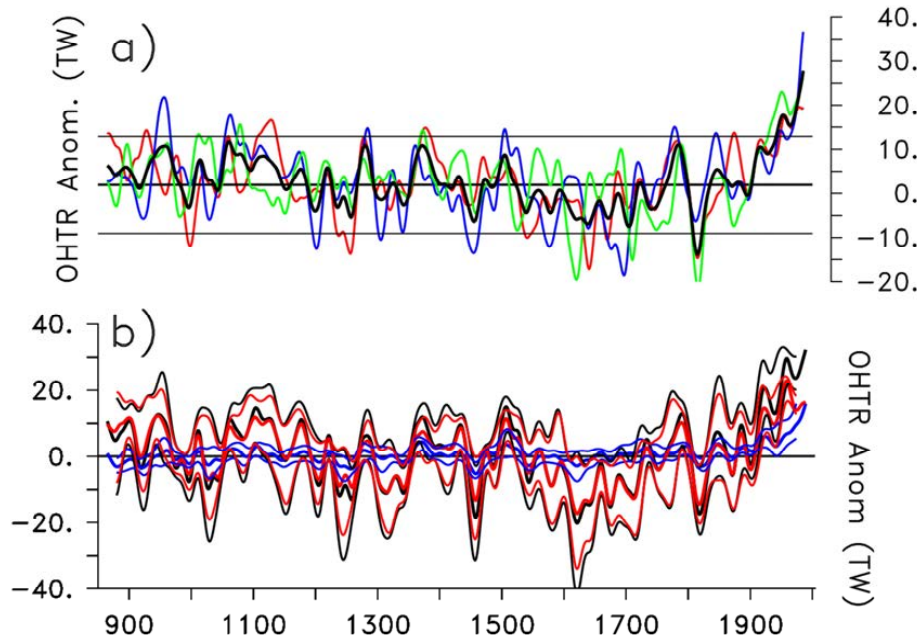


Figure 2. (a) Simulated ocean heat transport (OHTR) to the Arctic (combined OHTR through Fram Strait and Barents Sea Opening) as anomalies w.r.t. the pre-industrial mean; colored lines indicate individual simulations pr1, pr2 and pr3, and the solid black line is the ensemble mean. (b) Total OHTR (TOHTR, black lines) averaged over 60–65° N, subdivided into gyre-related OHTR (red, GOHTR), and overturning-circulation-related OHTR (blue, MOHTR). The thick lines represent the ensemble mean and the thin lines the ensemble spread for each quantity. All time-series were smoothed by a 31 yr running mean. Units are TW (1 TW = 10^{12} Watt).

Simulating enhanced modern heat transfer to the Arctic

J. H. Jungclaus et al.

Title Page

Abstract

Introduction

Conclusions

References

Tables

Figures



Back

Close

Full Screen / Esc

Printer-friendly Version

Interactive Discussion



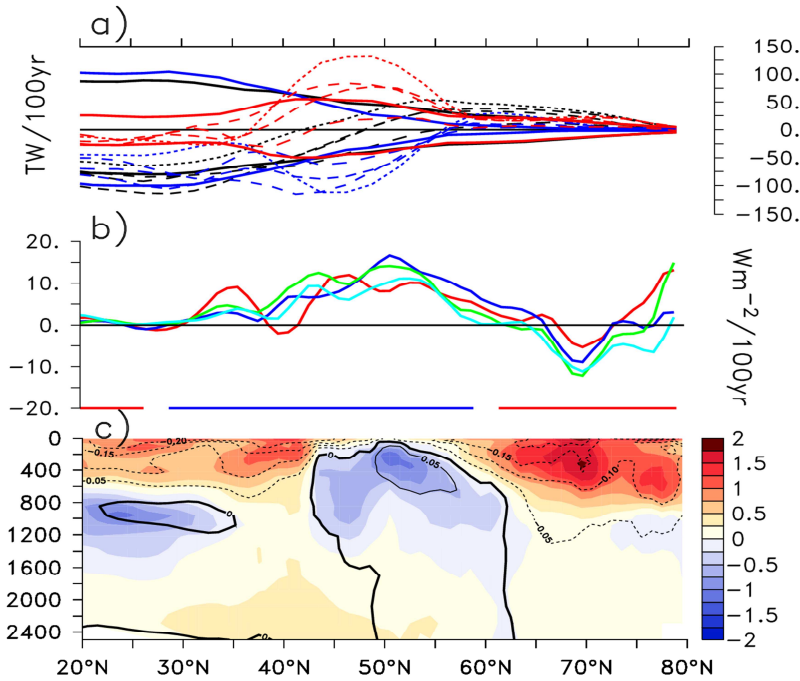


Figure 3. Simulated (experiments pr1, pr2, pr3, and hr1) 20th century linear trends (1905–2005) as zonal averages over the Atlantic basin: **(a)** (black dashed lines) TOHTR, (red dashed lines) GOHTR, and (blue dashed lines) MOHTR. Solid lines of respective color bracketing the zero line indicate the 5–95%-ile ranges of centennial trends in the unperturbed PiCtrl experiment. **(b)** Atmosphere–ocean heat fluxes (positive values indicate increased heat transfer from the atmosphere to the ocean or cooling of the atmosphere by the ocean). Colored lines are individual simulations, blue and red horizontal lines at the bottom of the plot indicate regions, where the ensemble-mean TOHTR divergence is positive (cooling by lateral advection) or negative (warming by lateral advection). **(c)** Temperature (color shading) and density (contours, contour interval 0.05 $kg\ m^{-3}$) trends from the pr2 experiment.

Simulating enhanced modern heat transfer to the Arctic

J. H. Jungclaus et al.

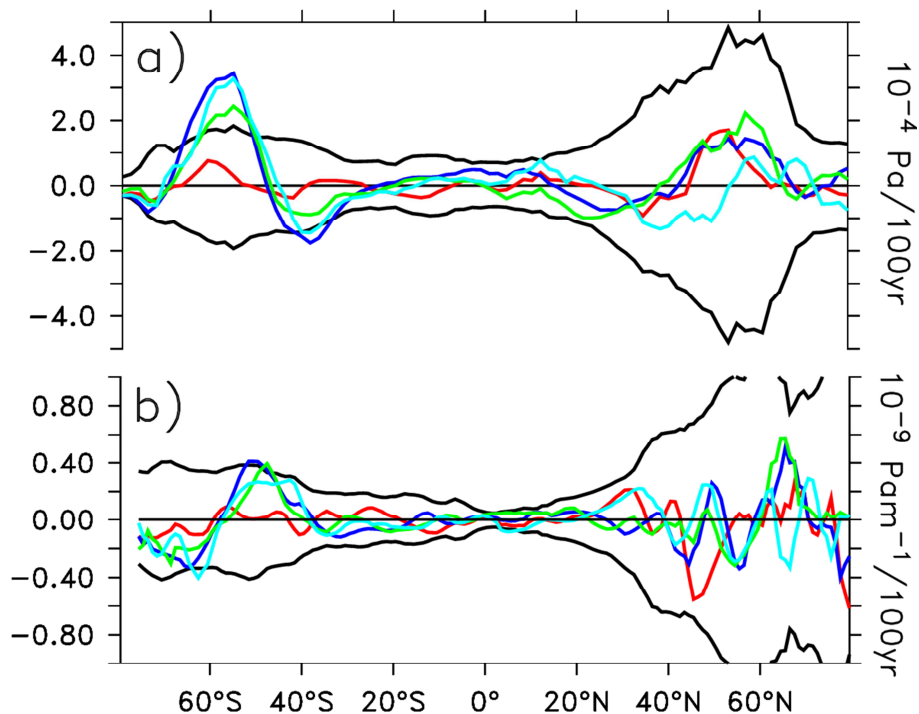


Figure 4. Simulated (experiments pr1, pr2, pr3, and hr1) 20th century linear trends (1905–2005) as zonal averages over the Atlantic basin of **(a)** wind stress (units $10^{-2} \text{ Pa} (100 \text{ yr})^{-1}$) and **(b)** wind stress curl (in $10^{-9} \text{ Pa m}^{-1} (100 \text{ yr})^{-1}$). Colored lines denote the experiments pr1, pr2, pr3, and hr1 and black lines bracketing the zero line show the 5–95 %-ile range of centennial trends in the unperturbed PiCtrl experiment.

Title Page

Abstract

Introduction

Conclusions

References

Tables

Figures



Back

Close

Full Screen / Esc

Printer-friendly Version

Interactive Discussion



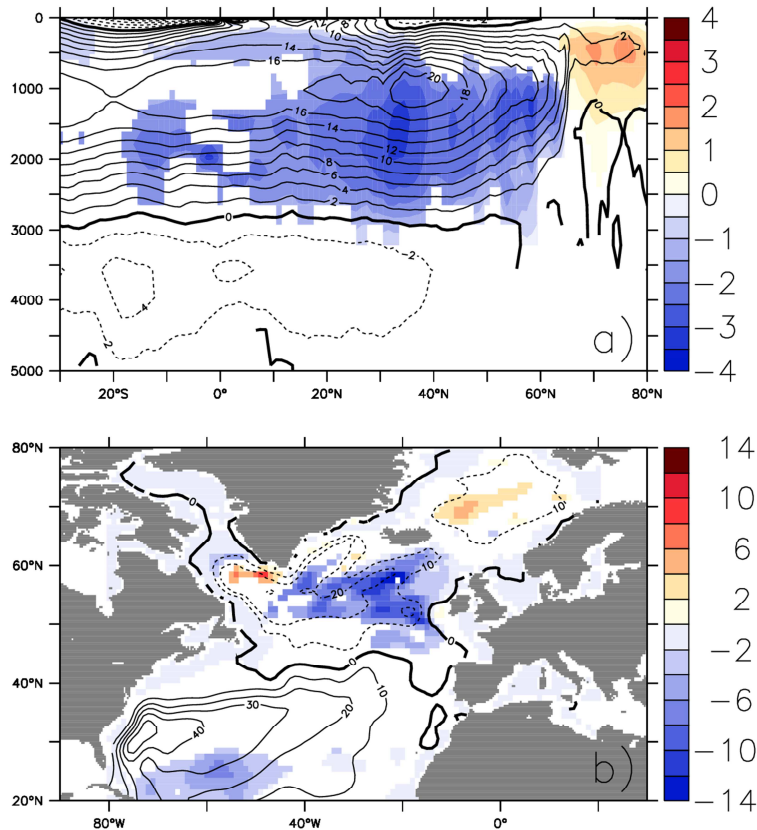


Figure 5. Simulated 20th century linear trends (1905–2005) in the pr2 simulation (color shading) of **(a)** meridional overturning circulation, and **(b)** barotropic stream function in the North Atlantic. Units are Sverdrups per 100 yr ($1 \text{ Sv} = 10^6 \text{ m}^3 \text{ s}^{-1}$). Contour lines (contour intervals 2 Sv for overturning and 10 Sv for barotropic stream function) describe the pre-industrial mean state. In both panels, only anomalies are shown that exceed the 5–95 %-ile range of centennial trends derived from the PiCtrl simulations.

Simulating enhanced modern heat transfer to the Arctic

J. H. Jungclaus et al.

Title Page

Abstract Introduction

Conclusions References

Tables Figures

◀ ▶

◀ ▶

Back Close

Full Screen / Esc

Printer-friendly Version

Interactive Discussion



Simulating enhanced modern heat transfer to the Arctic

J. H. Jungclaus et al.

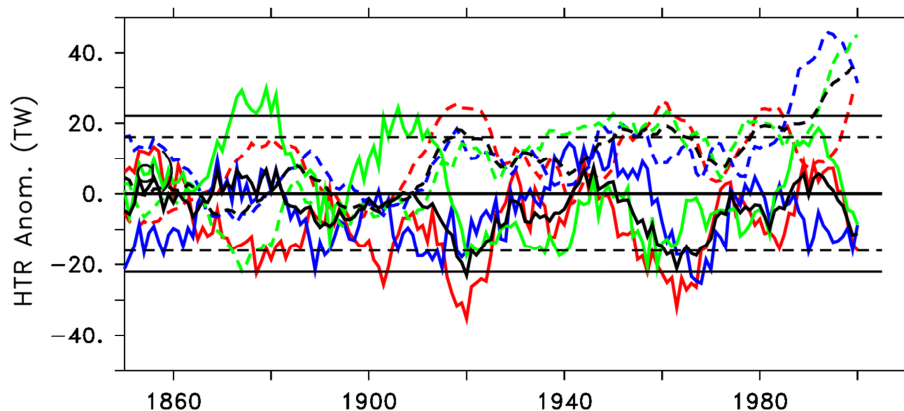


Figure 7. Time series of simulated (solid lines) atmospheric heat transports (AHTR) and (dashed lines) TOHTR at 70° N as anomalies w.r.t. the pre-industrial mean (colored lines for experiments pr1, pr2, pr3; time series shown as black dashed and solid lines denote the respective ensemble means). The horizontal black lines bracketing the zero lines are the respective 2- σ ranges derived from the PiCtrl experiment. An 11 yr running mean was applied to all data sets.

Title Page

Abstract

Introduction

Conclusions

References

Tables

Figures



Back

Close

Full Screen / Esc

Printer-friendly Version

Interactive Discussion

